



**HAL**  
open science

## Rheology of lime paste - A comparison with cement paste

Marine Fourmentin, Guillaume Ovarlez, Pamela Françoise Faure, Ulrike Peter, Didier Lesueur, Daniel Daviller, Philippe Coussot

► **To cite this version:**

Marine Fourmentin, Guillaume Ovarlez, Pamela Françoise Faure, Ulrike Peter, Didier Lesueur, et al.. Rheology of lime paste - A comparison with cement paste. *Rheologica Acta*, 2015, 54 (7), pp.647 - 656. 10.1007/s00397-015-0858-7 . hal-01784886

**HAL Id: hal-01784886**

**<https://enpc.hal.science/hal-01784886>**

Submitted on 3 May 2018

**HAL** is a multi-disciplinary open access archive for the deposit and dissemination of scientific research documents, whether they are published or not. The documents may come from teaching and research institutions in France or abroad, or from public or private research centers.

L'archive ouverte pluridisciplinaire **HAL**, est destinée au dépôt et à la diffusion de documents scientifiques de niveau recherche, publiés ou non, émanant des établissements d'enseignement et de recherche français ou étrangers, des laboratoires publics ou privés.

# Rheology of lime paste - A comparison with cement paste –

Marine Fourmentin, Guillaume Ovarlez, Paméla Faure, Ulrike Peter\*, Didier Lesueur\*\*, Daniel Daviller\*\*\*, Philippe Coussot

*Université Paris-Est, Laboratoire Navier (ENPC-IFSTTAR-CNRS), Champs sur Marne, France*

*\* LHOIST Recherche et Développement, Nivelles, Belgique*

*LHOIST, Paris, France*

*\*\*\* BCB, Lhoist, Besançon, France*

**Abstract:** The rheological properties of a suspension of lime in water (lime putty) are studied with the help of creep tests in a wide range of deformations including very small values. The results are compared with those obtained with a cement paste and several similarities between the two systems are observed. It is shown that the apparent yield stress of a lime suspension is the sum of two components: one due to standard reversible colloidal interactions and one due to the formation of a brittle structure associated with the formation of links due to dissolution-precipitation mechanisms. This second component increases with the time of rest as the square root of time, and the corresponding structure irreversibly breaks as soon as some significant deformation has been imposed. We show that similar structures are formed at concentrations between 25 and 34% (solid volume fraction) and evolve in a similar way when the time is scaled by a factor decreasing with the solid fraction.

## 1. Introduction

Lime has commonly been used as an aerial binder in mortars until the emergence of Portland cement in the middle of the 19<sup>th</sup> century. After the discovery of this new hydraulic binder, lime in the construction field was forsaken even though it has proved its flexibility and transfer properties. Besides, the physico-chemical or mechanical properties of cement pastes have been widely studied, but this is not the case for lime pastes. Hydrated lime ( $\text{Ca}(\text{OH})_2$ ), also named calcium hydroxide or portlandite) is obtained from calcination of calcareous rock, which leads to calcium oxide (quicklime). Quicklime is very reactive in the presence of water and is transformed to hydrated lime by a hydration reaction called slaking. Lime production techniques lead to the production of  $\text{Ca}(\text{OH})_2$  of different physico-chemical characteristics, depending on diverse factors as burning temperature, particle reactivity and slaking conditions (Boynton 1980).

Lime pastes or mortars used as construction materials must have specific rheological characteristics. Indeed they must be able to flow easily for a good handling, but they must also rapidly behave as solids after their laying to avoid particle sedimentation. This is possible because these materials are yield stress fluids, i.e. solids that are able to flow like liquids if submitted to a sufficiently high stress. The critical stress associated with this transition is the yield stress.

It is also known since 8000 BC that a lime paste evolves with time. Indeed the preparation mode consisted to slake quicklime in a large amount of water, isolate it from the atmosphere, and wait

for the mix to reach a creamy texture (Vitruvius 1914). According to the Roman practice, it was recommended to age lime pastes for at least three years before use. Although some of these evolutions are probably linked to the risk of slow hydration of overburnt limes, These evolutions were also proposed to be associated with complex microstructural changes in time (Mascolo et al. 2010, Rodriguez-Navarro et al. 1998). According to these studies,  $\text{Ca}(\text{OH})_2$  crystals undergo both significant morphologic changes (from prisms to platelike crystals) and particle-size reduction upon aging. The reason for this could lie in differences in solubility between the different faces of the crystal, in terms of in solubility and surface energies, associated with the presence of heterogeneous secondary nucleation of nanometer-scale platelike portlandite crystals on preexisting larger  $\text{Ca}(\text{OH})_2$  crystals (Mascolo et al. 2010, Rodriguez-Navarro et al. 1998, Arizzi et al. 2012, Ruiz-Agudo and Rodriguez-Navarro 2010). In parallel, the aging of a lime paste was shown to lead to a progressive strengthening of the material as observed by an increase of the apparent yield stress.

So far only a few studies focused on the rheology of lime pastes. Atzeni et al. (2004) followed the stress evolution in time (peak followed by decrease to a plateau) when imposing constant shear rates. They could identify the apparent yield stress of different types of lime putties and a “fluidification range” associated with the stress decrease phase. Finally they suggested that a Bingham model could represent the steady state shear stress vs shear rate data. Subsequent works focused on the impact of physico-chemical lime characteristics on some of these rheological parameters (Vavrova and Kotlik 2003). In particular it was shown that aged lime putties become more viscous. The most complete rheological study so far was probably that carried out by Ruiz-Agudo et al. (2010). They found that the flow curve of such systems cannot be easily identified since during a sweep test there is a significant hysteresis between the increasing and decreasing curve, which is related to a breakage of the structure. They also showed that the aging of these systems can be described through the increase of the apparent yield stress in time.

Lime putties are basically concentrated suspensions of solid particles in water. The effect of coarse (non-colloidal) particles is essentially to increase the viscosity. Colloidal interactions between small particles can lead to the formation of a network of links throughout the sample which must be broken for flow to take place, and which is at the origin of the yield stress (see Coussot (2014)). In the absence of chemical reactions these links break and form again if the sample is left at rest for some time. From a mechanical point of view this process is associated with a thixotropic behavior: the material exhibits a yield stress increasing with the time at rest; when a flow is imposed the structure breaks, so that the apparent viscosity decreases, but this breakage is reversible. At first sight such properties are consistent with those observed by Ruiz-Agudo and Rodriguez-Navarro (2010).

However, as mentioned earlier, in these systems changes of microstructure have also been observed to occur over long time and we can suspect that they start to develop over short time. In this context the question remains open as to whether the destructuring processes observed in rheological tests are reversible because they are mainly governed by colloidal interactions or irreversible because they are governed by chemical reactions. Our objective in this paper will thus be to clarify the effective rheological behavior of lime putties and as far as possible distinguish between reversible and irreversible effects from a careful mechanical characterization of the materials. Since the general trends above described are quite analogous to what can be expected for cement pastes, we will also compare the results with those obtained for a typical

cement paste. We start by describing the materials and methods (Section 2) then we present and analyze the data (Section 3).

## 2. Material and methods

### 2.1 Materials

### 2.1 Materials

We used a standard hydrated lime CL90 S (according to EN 459-1) provided by *Lhoist*, and a grey cement CEM I 52.5 N from *Vicat*. The composition of the hydrated lime was determined by thermogravimetric analysis (TGA) using a multiple sampling thermogravimetric analyzer TGA-2000 from Las Navas Instruments by a temperature ramp from 20°C to 950°C with a temperature increase of 5°C per minute. The chemical composition was then refined using Xray fluorescence (XRF) with a MagiX PRO PW 2540 from PANalytical. The mineralogical composition of the cement was analyzed by Xray diffraction (XRD) performing Rietveld refinement. The compositions are presented in Table 1. Table 2 shows selected physical properties. The specific surface area was measured for both materials by N<sub>2</sub> adsorption according to the Brunauer–Emmett–Teller theory (BET) using a TriStar from Micrometrics. The powder density was determined acc. to EN 459-2 (loose bulk density). As expected, hydrated lime had a BET specific surface area more than ten times larger than that of cement, and a lower density.

Component [wt%]	Method	Hydrated lime	Cement
Ca(OH) <sub>2</sub>	TGA	91.3	0.9
CaCO <sub>3</sub>	TGA	2.7	1.6
H <sub>2</sub> O	TGA	1.8	0.8
C <sub>3</sub> S	XRD		56.9
C <sub>2</sub> S	XRD		22.6
C <sub>3</sub> A	XRD		0.6
C <sub>4</sub> AF	XRD		14.8
CaSO <sub>4</sub> ·2H <sub>2</sub> O	XRD		1.7
CaO	XRF	2.51	
MgO	XRF	0.59	
SiO <sub>2</sub>	XRF	0.58	
Al <sub>2</sub> O <sub>3</sub>	XRF	0.25	
SO <sub>3</sub>	XRF	0.06	

**Table 1:** Main components of the studied materials, as determined by XRD, XRF and TGA

Component [wt%]	Method	Hydrated lime	Cement
Specific surface area [m <sup>2</sup> /g]	BET	15.1	1.3
Powder density [kg/m <sup>3</sup> ]	EN 459-2		

**Table 2:** Main physical characteristics of the studied materials: specific surface area (BET) and powder density

The particle size distribution was measured by light scattering on a Coulter LS 13320 in methanol. Since hydrated lime has a tendency to aggregate, which can lead to an overestimation of the particle size, the sample was first submitted to ultrasound during one minute (Sonics - 850W). The cement exhibited a particle size distribution (see Figure 1) spreading from 1 to 50  $\mu\text{m}$  with a mean size around 10  $\mu\text{m}$  while the hydrated lime contained particles in the range 1 to 10  $\mu\text{m}$  with an average size around 4  $\mu\text{m}$ .

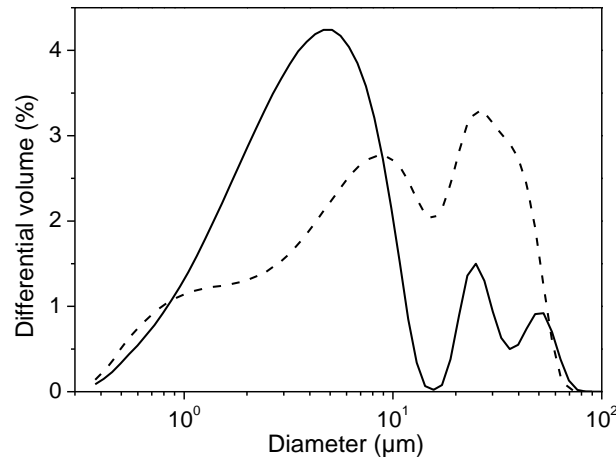


**Figure 1:** Particle size distribution of raw materials: hydrated lime (continuous line) and cement (dashed line).

The pastes were prepared by pouring the material powder in water, then mixing by hand for one minute and at 600 rpm with a mechanical mixer for another minute. Each step was precisely timed until the pastes were cast for rheological measurements. Such a protocol allows for a very good repeatability despite the fast evolution of the properties of these materials with time.

A single water to solid ratio (in weight) of 0.4 was used for the cement paste, which corresponds to a solid volume fraction ( $\phi$ ) of 44%. For the lime this ratio was varied between 0.87 and 1.35 which, with a typical particle density of 2.2 g/cm<sup>3</sup>, corresponds to solid volume fraction between 25 and 34%. In these ranges of concentrations our samples appear to be “pasty” materials, i.e. a volume of the order of a few milliliters keeps the shape it has been given when it is left at rest under its own weight, but can flow when a sufficiently larger stress is imposed to it.

## 2.2 Rheometry

We used a C-VOR Bohlin® rheometer with imposed stress. The Vane geometry is a six-bladed paddle with a diameter of 25 mm. The cup is 37 mm of diameter and 60 mm depth. The gap between the inner and outer tools (i.e. 6 mm) is much larger than the maximum particle size so that we expect the continuum assumption is valid in this context. The cup was covered with sand paper to avoid any problem of wall slip. The validity of this geometry to carry out relevant rheometrical tests with yield stress fluids was discussed by Nguyen and Boger (1985) and Ovarlez et al (2011). **In particular, flow fields with linear and nonlinear materials are more**

**complex (bidimensional) in this geometry than with a coaxial cylinder (Ovarlez et al (2011)), which makes it difficult to obtain an absolute determination of the value of the material's rheological properties. Moreover when the stress is larger but close to the yield stress some part of the fluid near the outer cylinder may be unsheared.** This implies that the basic calculation for the shear rate, which is obtained from the ratio of the rotation velocity to the gap, is underestimated. This possible effect must be kept in mind in the analysis of the data.

With such time-dependent materials the preparation of the sample is critical since it already involves some flow history of the material which may have an impact on its subsequent behavior. In order to reach good repeatability of results, a precise protocol was used. After preparation and mixing, the paste is put into the cup of the rheometer and the vane tool is introduced at a precise timing. The sample is then pre-sheared during 1 min. at  $100\text{ s}^{-1}$  and left at rest some well-defined time before starting the specific rheometrical test. With such a protocol an excellent repeatability (to within 3%) of data was obtained, for example in the case of creep tests, for different samples with the same preparation. This ensures the relevance of the subsequent study of different parameters such as the rest period or the paste concentration.

We carried out different types of rheometrical tests, namely sweep tests (from 0 to 130 Pa), oscillations (at a frequency of 1 Hz and different amplitudes of deformations), and creep tests under controlled velocity at two low shear rates ( $10^{-2}\text{ s}^{-1}$  and  $3.10^{-4}\text{ s}^{-1}$ ). The procedures are also described in more details in the text because they are intimately linked to the rheological properties which are explored.

### 3. Results and discussion

#### 3.1 Flow curve

We started rheometrical tests by the basic one for appreciating the overall behavior of a complex fluid. It consists to apply an increasing (logarithmic) ramp of shear rate from 0 to 130 Pa followed by a decreasing ramp towards zero. This makes it possible to get, from a simple and rapid test, a view of the rheological behavior over a wide range of flow conditions. Here after the preshear the materials were left at rest for 5 min. (lime) or 1 min. (cement) and the increasing and decreasing ramps lasted 2 min.

A typical result is shown in Figure 2. We observe an initial rapid increase of the shear stress with shear rate before reaching a stress plateau. This trend is usually found for yield stress fluids. In the initial stage, after the rest, the material is in a solid regime: the increase of shear rate at low values over relatively short duration corresponds to small deformations, so that the material remains some time in its solid regime. The corresponding stress rapidly increases as the deformation increases. This part of the flow curve varies with the rate of increase of the imposed shear rate. Then the plateau corresponds to the transition between the solid and the liquid regime: the plateau level may be considered as the “static” yield stress of the material. At larger shear rates in the liquid regime the stress significantly increases with the shear rate. During the decreasing ramp the stress is situated significantly below the increasing curve, which suggests that thixotropic effects exist: the apparent viscosity decreases with the flow duration. Finally the

decreasing curve ends by a stress plateau, which may be considered as the “dynamic” yield stress. In fact, for a thixotropic material, the static and dynamic yield stresses depend on the previous flow history and the timing of the sweep test (Coussot 2014).

Under these conditions it is likely that the data for the decreasing curve are the closest to the effective flow curve of the material, i.e. in steady state flow conditions. As usual for yield stress fluids these data can be well represented by a Herschel-Bulkley (HB) model over 4-5 decades of shear rates (see Figure 2a):  $\tau < \tau_c \Rightarrow \dot{\gamma} = 0$  (solid regime);  $\tau > \tau_c \Rightarrow \tau = \tau_c + k\dot{\gamma}^n$  (liquid regime), in which  $\tau$  is the shear stress amplitude,  $\dot{\gamma}$  the shear rate amplitude,  $\tau_c$  the yield stress and  $k$  and  $n$  two material parameters. Note that there is a discrepancy of the model with data at very low shear rates but it is likely that in this range some time-dependent shear rate heterogeneity can play a significant role on the apparent flow characteristics.

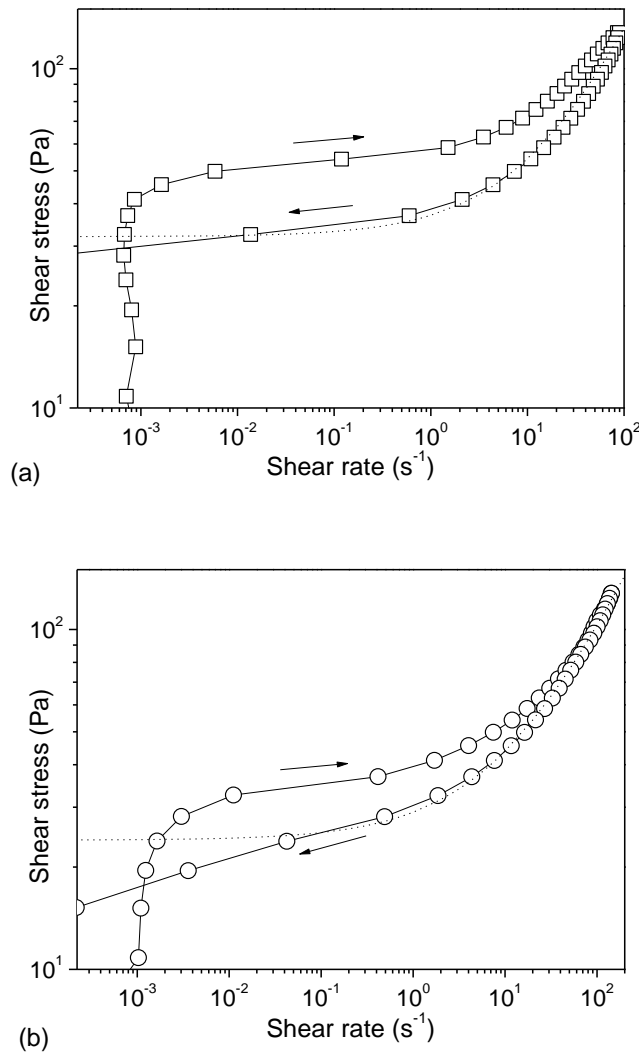


**Figure 2:** Apparent flow curve obtained from a shear rate sweep for: (a) a lime paste immediately after preparation with a water to lime ratio of 1.17; (b) a cement paste with a water to cement ratio of 0.4 by weight. The dotted line corresponds to a Herschel-Bulkley model fitted to data for the

decreasing shear rate ramp with the following parameter values: (lime paste)  $\tau_c = 40 \text{ Pa}$  ,  
 $k = 5 \text{ Pa.s}^n$  ,  $n = 0.65$  ; (cement paste)  $\tau_c = 24 \text{ Pa}$  ,  $k = 5 \text{ Pa.s}^n$  ,  $n = 0.6$  ;

So as a first approximation a lime paste is a yield stress fluid well described by a simple rheological model, and exhibiting some destructuring during flow. A similar behavior is obtained with a cement paste (see Figure 2b). **Such materials are typically thixotropic yield stress fluids, for which it would be possible to study a variety of rheological characteristics as a function of flow history. However, considering the possible reversible and irreversible evolutions of the structure of the material and the possible resulting flow heterogeneities developing in such situation (see Section 2.2) (Jarny et al. 2005), it becomes rapidly complex to further attempt to characterize the material properties from such tests. As a consequence,** in the following, in order to study the structure evolution in time, we will focus on tests in which the flow regime and the state of the material are better controlled at any time during the test.

**Looking at the flow curves it is remarkable that the apparent flow curve obtained from the decreasing ramp can be represented by a HB model with a set of rheological parameters which are not very different ( (see Figure 2): slightly different values of the yield stress to consistency ratio but similar value of the exponent.** This means that as soon as they are almost flowing steadily a cement and a lime paste exhibit the same type of rheological behavior.

### 3.2 Solid-liquid transition

Here we focus on the solid regime and the solid-liquid transition through creep flows at low shear rates starting from the material at rest. By this means we can follow the stress as a function of the deformation imposed to the material when viscous effects induced by the shear rate are negligible.

A typical result under such conditions is shown in Figure 3: the stress progressively increases up to a maximum as the deformation increases up to a critical value, then it drops and finally tends (over our range of observation of the deformation) to a plateau situated at a significantly lower level. Such a result is consistent with the hysteresis loop in the sweep test (see above) and is typical of time-dependent materials. It reflects the fact that the material exhibits a structure which is associated with its apparent (static) yield stress and breaks beyond some critical deformation (here about 0.04). But because the rate of restructuring is not rapid enough, the stress needed to maintain flow (at larger deformations) decreases, as the structure progressively further breaks.

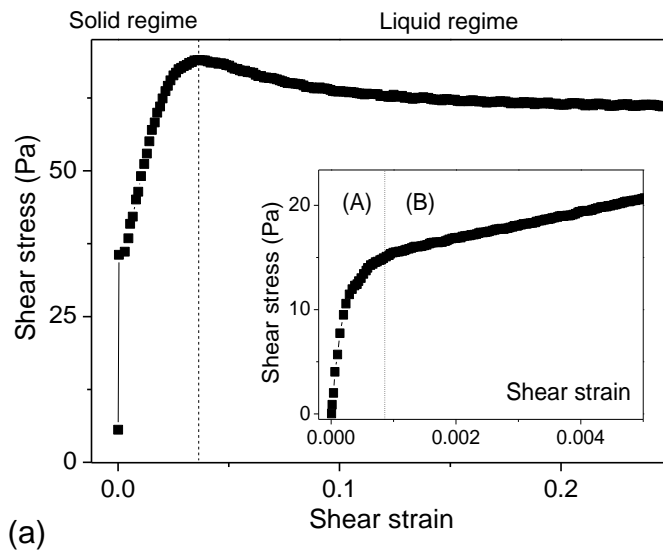
The stress curve below the yield stress (solid regime region in Figure 3) has a shape which differs from the usual one with simple yield stress fluids (see for example Coussot et al. 2006) for which the stress vs strain slope is constant over a significant strain range starting from zero. Here the slope seems to decrease significantly beyond some small deformation (see Figure 3), which makes it difficult to determine the shear modulus of the material in its solid regime. This



suggests that the material exhibits some behavior change around some second critical deformation far below the critical deformation associated with the solid-liquid transition. As a consequence we studied the behavior of the material in such creep tests at two different shear rates ( $10^{-2} \text{ s}^{-1}$  and  $3 \cdot 10^{-4} \text{ s}^{-1}$ ), which provides information about the material behavior in two very different ranges of deformation.

From such tests we see that the stress increase in the solid regime up to the yield stress occurs in two steps: first we have an increase up to a value of the order of 15 Pa with a very steep slope. The critical strain for this step is 0.1 %; then we have a second increase with a much smaller slope. The critical strain for this step is of the order of a few %. A similar trend is observed for a cement paste (see Figure 3b) as already remarked by Roussel et al. (2012) for other cement pastes. Here we see that with a lime paste this effect occurs after a longer time of rest (see Figure 3a) and with a slightly larger critical strain for the first step (around 0.1%).

These trends, which are quite different from those observed with simple yield stress fluids, mean that these pastes have two types of structures which are at the origin of the yield stress and which successively break when the deformation increases. At small deformation this is essentially a structure with a high shear modulus and a very small critical strain which is at the origin of the stress increase. We thus have a brittle structure which rapidly breaks. Then a softer structure with a lower shear modulus and larger critical strain is deformed.



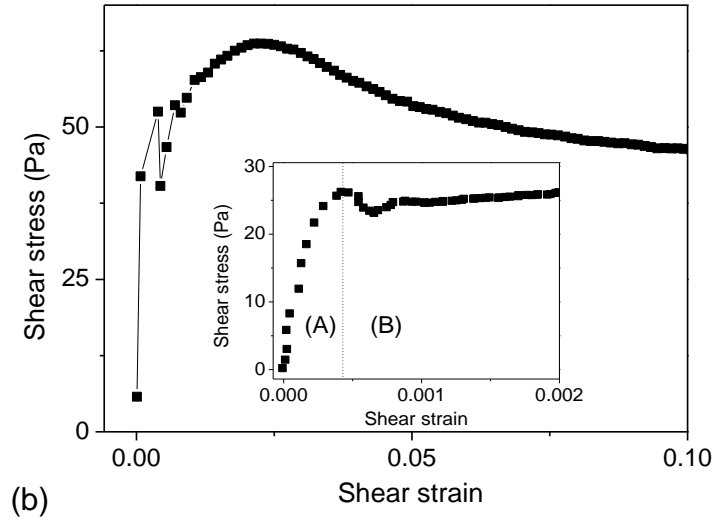


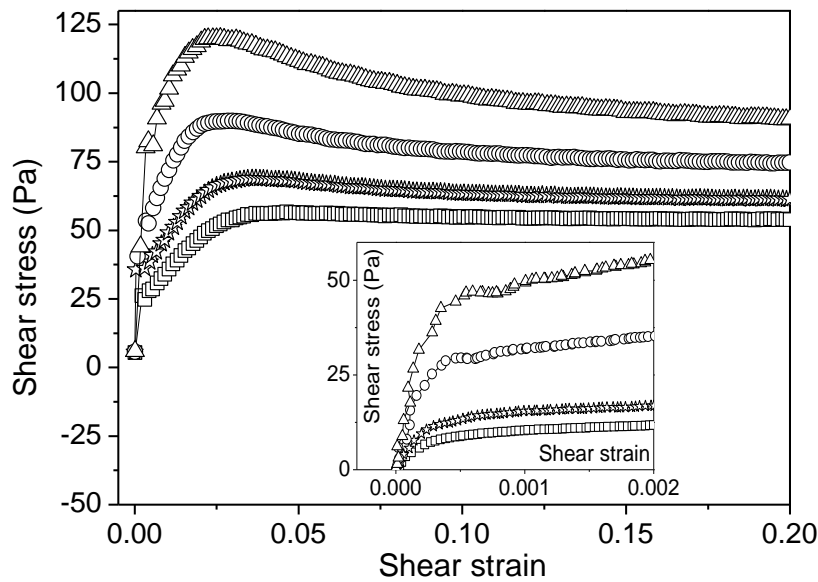
**Figure 3:** Shear stress as a function of shear strain during a creep test at high shear rate ( $10^{-2} \text{ s}^{-1}$ ) or low shear rate ( $3 \cdot 10^{-4} \text{ s}^{-1}$ ) (inset) for: (a) a lime paste (water to lime ratio of 1.3) after 20 min. of rest, and (b) a cement paste (water to cement ratio of 0.4) after 2 min of rest. The vertical dotted line in the inset shows the position of the transition between the first and the second structure (see text).

### 3.3 The different structures in the solid regime

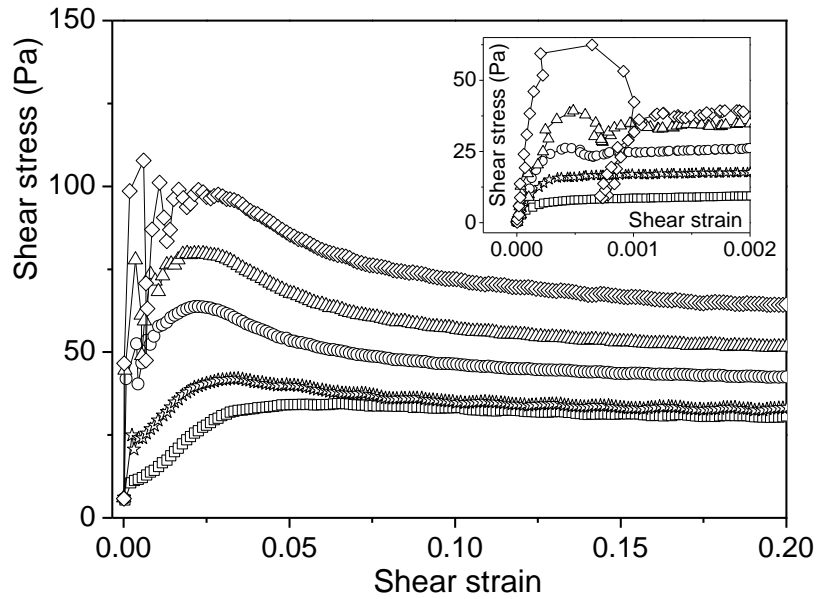
The above measurements show that there exist two types of structures which are at the origin of the solid regime but do not provide clear information concerning the respective contribution of each of the structures to the static yield stress of the material. A further insight in this problem is provided by data from the same test after different times of rest. We see that now the stress vs strain curve evolves, in particular the main peak height increases with the time of rest (see Figure 4). In parallel the critical stress associated with the brittle structure increases (see inset of Figure 4). It is interesting to compare the evolution of the main peak value and that associated with the first structure breakage, i.e. the stress at the slope breakage at very low deformation. We observe that for both material types (see Figure 5) these two values approximately evolve parallel to each other.

The picture we get from these results is as follows, which is similar to that suggested for a cement paste (Roussel et al. 2012): the different pastes are basically concentrated suspensions of colloidal particles which may somewhat interact at distance and anyway form a “soft jammed structure”. Such a structure behaves approximately like an elastic solid below some critical strain which is generally situated between 5 and 50%. This jammed network does not significantly strengthen with the time at rest. In addition there is a brittle structure which forms because of direct contacts between grains throughout the sample. This brittle structure strengthens with the time at rest. When a sufficiently large deformation is imposed, the brittle structure is fully broken and the resistance to flow at very low shear rate is essentially that due to the soft structure.

In fact, for the lime this picture does not exactly correspond to our observations. The difference between the peak level and the critical stress for breaking the brittle structure somewhat increases with the time of rest (see Figure 5). This suggests that the yield stress associated with the soft structure also increases with the time of rest. This assumption is consistent with the observation that the plateau level observed at deformation around 1, **and which was attributed essentially to the stress needed to break colloidal interactions**, increases with the time of rest (see Figure 4). It is however difficult to interpret further the data for such large deformation because in this regime artefacts such as edge effects or shear heterogeneities may start to play a significant role. We can simply remark that the stress plateau increase with the time of rest is close to the increase of the difference between the peak and the first critical stress, which further confirms that the soft structure also strengthens with the time of rest.



(a)



(b)

**Figure 4:** Shear stress as a function of shear strain during creep tests at high shear rate ( $10^{-2} \text{ s}^{-1}$ ) or low shear rate ( $3 \cdot 10^{-4} \text{ s}^{-1}$ ) (inset) for (a) a lime paste (water to lime ratio of 1.3), and (b) a cement paste (water to cement ratio of 0.4) after different times of rest following preshear (from bottom to top): (lime) 10, 20, 40, and 80 min., (cement), 30 s, 2, 5, 10, and 20 min.

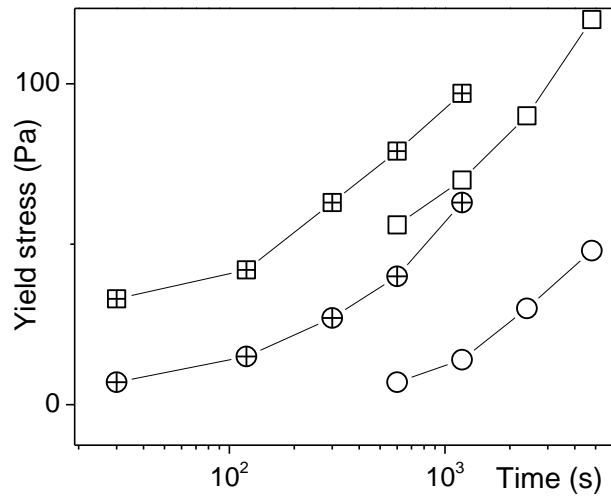


**Figure 5:** Critical stress associated with the transition between the first and second structure (circles) and stress peak (squares) for data of Figure 3 with a lime paste (open symbols) and a cement paste (crossed symbols).

### 3.4 Reversibility of the process

So far we have observed structuring processes which are usually described within the frame of thixotropy of complex fluids. However for each test at a different time of rest a new sample was used. In fact thixotropy is basically defined as a reversible phenomenon, which means that whatever the initial state of the material, if it is strongly sheared, it will afterwards forget its previous history and should end up in the same state.

In order to check that effect, we carried out two measurements on the same material: preshear just after set up, then a relatively short time of rest  $t$  followed by a creep test, then a long time of rest  $T > t$ , then again a strong preshear and a rest time  $t$  before a new creep test. Thus the material is submitted to the same test (preshear + rest + creep flow) at two times separated by a time at rest  $T$ . If the material was simply thixotropic we would get the same response in both creep tests, since it would have forgotten its flow history during the preshear.

In Figure 6 we see that this is not the case at least for significant times of rest (say larger than several tenths of minutes): the creep curve for the second test is significantly below the first one; the solid-liquid transition in the second test is much smoother, i.e. there is almost no stress peak. This effect is more marked for the lime paste than for the cement paste: the difference between the two stress levels in (approximately) steady state flow is about 23 Pa for the former and 7 Pa for the latter. This means that the structure formed during the initial period of rest after preparation (including preshear) has been partly broken definitively during the first creep test and the second preshear period. This irreversible part thus corresponds to some chemical effects (see below) on the interactions between particles which have an impact on the strength of the solid structure. It is natural to consider that these correspond to links between particles which are able to form during some time but can be definitively broken when the material flows. It is also worth emphasizing that the part of the structure which does not recover after preshear is essentially related to the brittle structure described above and which evolves during rest. This is proved by the fact that the difference between the two curves either in Figure 6a or in Figure 6b corresponds approximately to the difference in the initial stress step at very low deformation (insets figures 3).

For a cement paste this can be explained by hydration effects typically taking place in this time range. For the lime paste this could be explained by a dissolution precipitation mechanism, which would progressively weld the grains to each other. In this case, re-precipitated portlandite crystals are at the origin of the first critical strain visible on the creep curve (see Fig. 6a). Then a change of crystalline structure of portlandite seems to occur in a lime putty, as prismatic portlandite crystals change to platelike ones (Mascolo et al. 2010, Rodriguez-Navarro et al. 1998, Arizzi et al. 2012, Ruiz-Agudo and Rodriguez-Navarro 2010), which can be at the origin of the evolutions of the colloidal interactions in the mix.

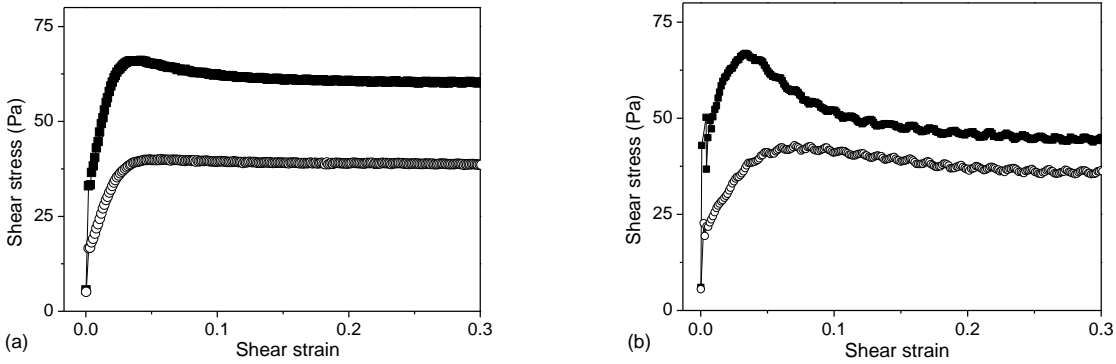


**Figure 6:** Shear stress as a function of shear strain during creep tests at high shear rate ( $10^{-2} \text{ s}^{-1}$ ) for: (a) a lime paste (water to lime ratio of 1.3) 20 min. after preshear following preparation (filled squares), and for the same test 1 h after the first one; (b) a cement paste (water to cement ratio of 0.4) 5 min. after preshear following preparation (filled squares), and for the same test 40 min. after the first one.

### 3.5 Structure evolution in time

In order to have get a more precise view of the structure evolution in time it is more appropriate to carry out oscillation tests. Let us first look at the response of the material when it is submitted to oscillations at an increasing deformation amplitude. For very low deformation the elastic and loss moduli are very high (see Figure 7), which contrasts with usual values (typically between 100 and 1000 Pa) observed for other yield stress materials that can easily be mixed by hand. This high moduli in fact correspond to the strength of the brittle structure identified above. Indeed, in this range of very small deformations, a rough estimate of the apparent elastic modulus from the ratio of stress to deformation in one of the above creep tests provides values close to the values here obtained (see Figure 7). Beyond some critical deformation (around  $5 \cdot 10^{-4}$ ) the two moduli collapse to much lower values, which corresponds to the breakage of the brittle structure observed in creep tests around the same critical deformation (see Figure 4). Then they go on decreasing for larger deformations and reach values of the order of 100 Pa which are values typically observed for soft-jammed systems, i.e. materials for which the yield stress is essentially due to the jamming of particles with soft interactions in a given liquid volume.

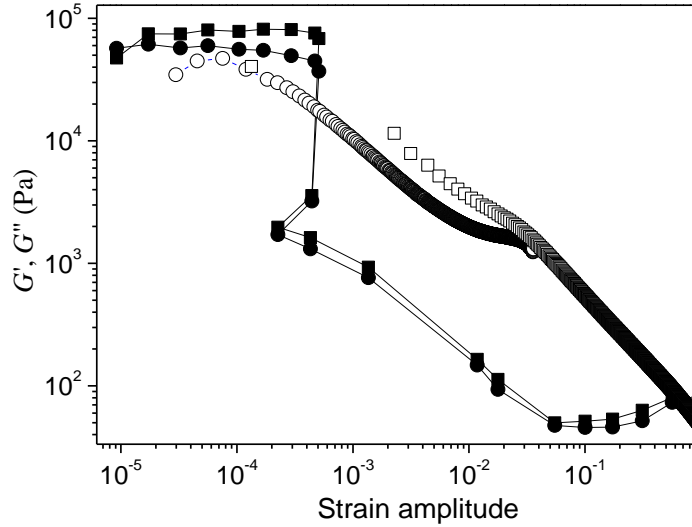


**Figure 7:** Elastic (filled symbols) and loss (open symbols) moduli measured as a function of strain amplitude (frequency 1 Hz) for a lime paste ( $\phi = 28\%$ ) (two tests on different samples of the same material (squares and circles)).

Now that we have seen that the brittle structure is mainly responsible for the evolution in time, we can focus on the evolution of the elastic modulus measured at very low deformation (i.e. below  $5 \cdot 10^{-4}$ ). For these measurements, the set up protocol is the same as for creep curve measurements, except that there is no resting period after the preshear. A typical example of such data is shown in Figure 8 for a cement paste and a lime paste. First we can check that the elastic modulus measured with oscillations corresponds to the one which could be deduced from creep tests (from the slope of the stress vs strain curve at very low deformation, see fig. 3). It appears that the two set of data at different resting times match globally well. There remains some discrepancy, which may be due to viscoelastic effects in the solid regime so that two different techniques can provide different values of the apparent elastic modulus. In this context the critical result is that the evolution in time of the two values are similar.

From dynamic tests we now have a continuous information on the evolution of the elastic modulus over a wide range of times. For both material types the elastic modulus significantly increases in time: it increases by a factor about 50 over a period of 15 hours. Roughly speaking this increase scales as  $\sqrt{t}$ , since the curves are more or less parallel to the line of slope  $\frac{1}{2}$  (see Figure 8). The increase is not regular, i.e. the curves include a kind of step during which the elastic modulus suddenly increases very rapidly. We have no explanation for this step (which cannot be due to an apparatus artefact).

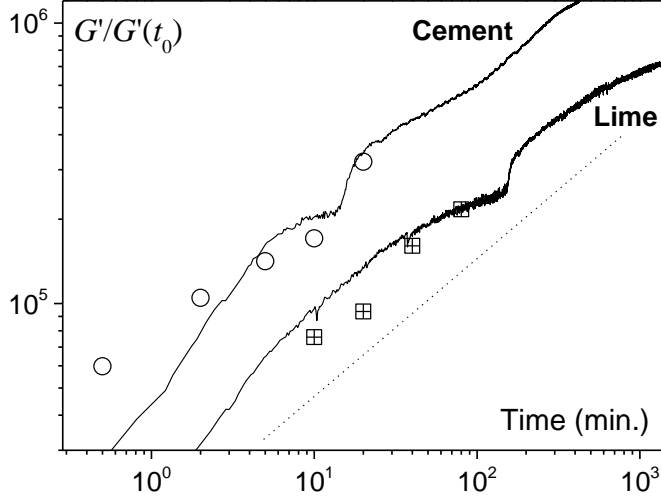


**Figure 8:** Elastic modulus in time measured from dynamic tests (continuous lines) at a frequency of 0.5Hz and comparison with data from creep tests at low shear rate ( $3.10^{-4} \text{ s}^{-1}$ ) for a lime paste ( $\phi = 28\%$ , crossed squares) and a cement paste ( $\phi = 44\%$ , circles). The dotted line of slope 1/2 is a guide for the eye.

In view of understanding the origin of this behavior it may be useful to look at the variation of the elastic modulus vs time curves when the solid fraction ( $\phi$ ) of the paste is varied (see Figure 9). The first observation is that at a given time  $G$  increases with  $\phi$ . This result is expected: for the same progress duration of chemical reaction, as the solid fraction increases, the number of contacts between particles increases and thus the strength of the network. However, the  $G(t)$  are not simply proportional by a single factor depending on  $\phi$ . The different curves are similar but are proportional by a time factor. This clearly appears from the position of the step, which is simply shifted towards shorter time as the solid fraction is increased. Under these conditions it is possible to plot all the data along a master curve by scaling the time by a factor ( $t_\phi$ ) which depends on the solid fraction (see Figure 10). This means that the elastic modulus may be written as

$$G(t, \phi) = G_0 f(t/t_\phi) \quad (1)$$

in which  $G_0$  is a constant and  $f$  a given function. Such a behavior is reminiscent of the aging behavior observed for thixotropic colloidal systems at different temperatures or concentrations (Ovarlez and Coussot 2007, Joshi et al. 2008).

This result could be explained by the following physical scheme. Our basic assumption is that due to the specific process at the origin of the creation of a structure (i.e. dissolution-precipitation) the material at a given solid fraction constitutes (in particular via its specific surface and the free volume it offers) a source of new elements which create this structure. Under these conditions, for a solid fraction  $\phi$ , after a time  $t_\phi$  a certain amount of elements has been created, which gives rise to a structure of strength  $G_0$ . Then the evolution in time of the strength



may be written in the form  $G_0 f(t/t_\phi)$ . For a solid fraction  $\phi'$  a structure with the same strength is reached at a time  $t_\phi$ , due to the creation of another amount of elements. For the solid fraction  $\phi$  after a time  $\lambda t_\phi$  a larger amount of elements has been created leading to a strength  $G_0 f(\lambda)$ . For the solid fraction  $\phi'$ , at a time  $\lambda t_\phi$  the amount of elements created has been increased by the same factor. Assuming the similarity of the two structures we deduce that the strength has also reached the value  $G_0 f(\lambda)$ . Applying this reasoning to any value  $\lambda$  leads to equation (1). Obviously such a picture remains essentially conceptual and a full modelling would require a more detailed analysis of the structure at a local scale.

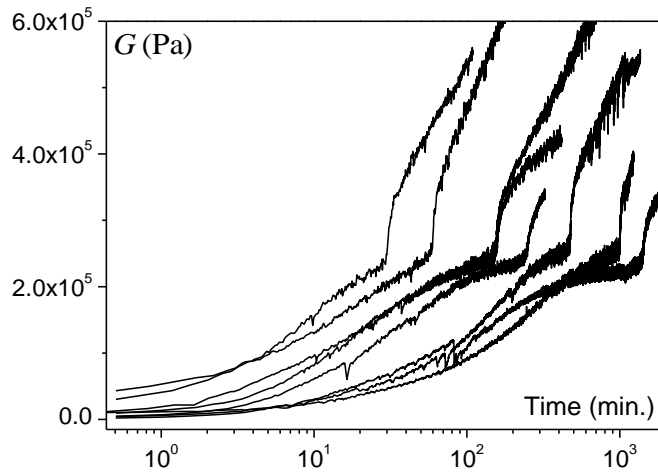


**Figure 9:** Elastic modulus as a function of time for lime pastes at different solid volume fractions: (from left to right) 34, 31, 29.5, 28, 27.5, 27, 26, 25%.

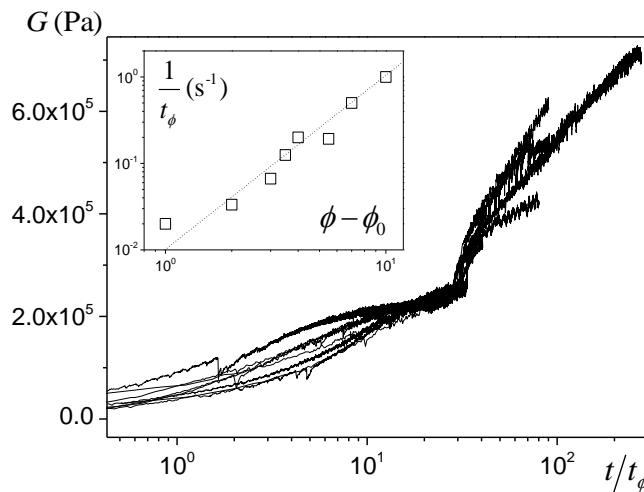


**Figure 10:** Elastic modulus for lime pastes at different solid volume fractions (data of Figure 9) as a function of the time rescaled by the characteristic time  $t_\phi$  (see text). The inset shows the variation of this parameter with the solid fraction. The dotted line in the inset has a slope  $1/2$ .

The variation of  $t_\phi$  with the solid fraction (see inset of Figure 10) can be represented by a model of the form  $1/t_\phi \propto (\phi - \phi_0)^2$ . Here  $\phi_0$  is the solid volume fraction for which we got a suspension which does not seem to have a yield stress. Thus it can be suggested that this concentration corresponds to the percolation threshold beyond which one starts to have a solid network which then reinforces in time.

#### 4. Conclusion

We have shown that lime pastes are yield stress fluids with a strong impact of time effects. Just after preparation they may be seen essentially as simple yield stress fluids, with a flow curve well represented by a Herschel-Bulkley model and no time-effects. As soon as they have been left at rest some time they exhibit a higher yield stress due to the formation of a brittle structure of links between grains. If this structure is broken the material behavior is close to that before rest. The yield stress associated with this brittle structure increases with the time of rest. The comparison with cement pastes strongly suggests that this results from dissolution-precipitation processes leading to the formation of links between grains. When such links are broken during the paste deformation they will not recover.

In practice this means that a higher stress is needed to break the brittle structure in the very first times of flow but as soon as the material has been slightly deformed it has lost a significant part of this yield stress and will flow under much lower stress. However this high initial yield stress allows the material to remain at rest (solid) under relatively high stress.

We could follow the evolution of this yield stress in time through the elastic modulus associated with very small deformations. It appears that this elastic modulus increases with the square root of time. Moreover the evolutions for different solid volume fractions were shown to be similar when the time is rescaled by a time factor, which provides a practical means for predicting the evolution for any solid fraction.

#### References

- Arizzi A, Hendrickx R, Cultrone G, Van Balen K (2012) Differences in the rheological properties of calcitic and dolimitic lime slurries, *Materiales de Construccion*, 62:231-250
- Atzeni C, Farci A, Floris D, and Meloni P (2004) Effect of Aging on Rheological Properties of Lime Putty, *J. Am. Ceram. Soc.*, 87:1764–1766
- Boynton RS (1980) *Chemistry and technology of lime and limestone*, Wiley, New York
- Coussot P (2014) *Rheophysics – The matter in all its states*, Springer, Berlin
- Coussot P, Tabuteau H, Chateau X, Tocquer L, and Ovarlez G (2006) Aging and solid or liquid behavior in pastes, *J. Rheol.*, 50:975-994
- Jarny S, Roussel N, Rodts S, Bertrand F, Leroy R, Coussot P (2005) Rheological behavior of cement pastes from MRI velocimetry, *Cement Concrete Res.*, 35:1873-1881

- Joshi YM, Reddy GRK, Kulkarni AL, Kumar N, Chhabra RP (2008) Rheological behaviour of aqueous suspensions of laponite: new insights into the ageing phenomena, *Proc. Royal Soc. A – Math. Phys. Eng. Sci.*, 464:469-489
- Mascolo G, Mascolo MC, Vitale A, Marino O (2010), Microstructure evolution of lime putty upon aging, *J. Cryst. Growth*, 312:2363-2368
- Nguyen DN, Boger DV (1985) Direct yield stress measurement with the vane method, *J. Rheol.*, 29:335-347
- Ovarlez G, and Coussot P (2007) The physical age of soft-jammed systems, *Physical Review E* 76, 011406
- Ovarlez G, Mahaut F, Bertrand F, Chateau X (2011) Flows and heterogeneities with a vane tool: Magnetic resonance imaging measurements, *J. Rheol.*, 55:197-223
- Rodriguez-Navarro CR, Hansen E, and Ginell WS (1998) Calcium Hydroxide Crystal Evolution upon Aging of Lime Putty, *J. Am. Ceram. Soc.*, 81:3032–3034
- Roussel N, Ovarlez G, Garrault S, and Brumaud C (2012) The origins of thixotropy of fresh cement pastes, *Cem. Concr. Res.*, 42:148-157 (2012)
- Ruiz-Agudo E, and Rodriguez-Navarro C (2010) Microstructure and Rheology of Lime Putty, *Langmuir*, 26:3868–3877
- Vavrova P, Kotlik P (2003) Rheological properties of lime putty, *Meterialy Pro Stavbu*, 3:6
- Vitruvius (1914) *The Ten Books of Architecture*. English translation by M. H. Morgan. Dover, New York